Evolution of equatorial irregularities under varying electrodynamical conditions: A multitechnique case study from Indian longitude zone

R. Hajra,[1] S. K. Chakraborty,[1] S. Mazumdar,[1] and S. Alex[2]

Received 6 April 2012; revised 30 May 2012; accepted 9 July 2012; published 28 August 2012.

[1] A comprehensive multitechnique study on the postsunset evolutions of equatorial ionization anomaly (EIA) and equatorial plasma density irregularities in the context of the varying electrodynamical conditions under normal equatorial electrojet (EEJ), complete and partial counter electrojet (CEJ) events is presented from the Indian longitude zone. The study involves analysis of scintillation data at VHF (250 MHz) and GPS L1 (1575.42 MHz) frequency, ionosonde data, magnetometer data along with global ionospheric maps (GIMs) of total electron content (TEC) for the vernal equinoctial months (March–April) of 2011. The investigation reveals inefficiency of the noontime peak EEJ to dictate the day-to-day variability of postsunset irregularity phenomena. Intensification of EEJ after ~1530 IST (Indian standard time) on normal EEJ days and significantly enhanced residual fields presumably due to CEJ event after ~1700 IST on complete and partial CEJ days are found to be associated with the resurgence of EIA and evolution of postsunset irregularities. The results are discussed in terms of superposition effects of electric fields arising from E- and F- region dynamos.

Citation: Hajra, R., S. K. Chakraborty, S. Mazumdar, and S. Alex (2012), Evolution of equatorial irregularities under varying electrodynamical conditions: A multitechnique case study from Indian longitude zone, *J. Geophys. Res.*, *117*, A08331, doi:10.1029/2012JA017808.

1. Introduction

[2] The distinct electrodynamical character of the magnetic equator leads to the most important features of the equatorial and low latitude ionosphere, namely (1) equatorial ionization anomaly (EIA) and (2) intense form of plasma density irregularities.

[3] The orthogonal configuration of the geomagnetic field ($\boldsymbol{B}$) and zonal electric field ($\boldsymbol{E}$) over the magnetic equator drives vertical $\boldsymbol{E} \times \boldsymbol{B}$ drift of ionospheric plasma to significantly high altitude, which subsequently diffuses along the highly conducting geomagnetic field lines due to gravitational and pressure gradient forces to the off-equatorial region on both sides of the magnetic equator. The processes, collectively known as "equatorial fountain" [*Martyn*, 1955; *Duncan*, 1960], result in a double humped latitudinal distribution of the ionization – a region of depleted ionization (ionization trough) at the magnetic equator and two crests of enhanced ionization around ±15–20° dip latitudes – known as EIA [*Appleton*, 1946]. It occurs over a large part of the day and extends well into the evening hours. On the other hand, plasma density irregularities develop near the magnetic equator mostly in the postsunset period. These are manifested by (1) bottomside spread echoes in the ionograms, (2) scintillations of the radio signals in the frequency range 100 MHz–4 GHz, (3) intensity bite-outs in the thermospheric airglow, (4) plume-like structures in the radar maps, and (5) depletion in plasma densities in the in situ satellite and rocket measurements. The generation/dynamics of the irregularities are known to vary with local time, season, solar and geomagnetic activities [*Booker and Wells*, 1938; *Woodman and LaHoz*, 1976; *DasGupta et al.*, 1985; *Basu et al.*, 2002; *Su et al.*, 2008; *Hajra et al.*, 2010; *Hajra and Chakraborty*, 2011].

[4] The primary driving mechanism of both the phenomena is largely dependent on the equatorial electrodynamics, modulated by equatorial electrojet (EEJ) and counter electrojet (CEJ) events. An enhanced ionospheric *E* region current flowing at 100 km altitude in the narrow latitude belt (~5° dip width) around the dip equator is referred to EEJ. It is produced by the global-scale daytime dynamo electric field in the presence of the horizontal magnetic field of the earth at the dip equator [*Cowling*, 1933; *Cowling and Borger*, 1948; *Chapman*, 1951]. At the ground level EEJ is manifested by large perturbation in the solar daily variation of the horizontal component (H) of the geomagnetic field. Sometimes EEJ current reverses from eastward to westward direction during morning and afternoon hours even on a magnetically quiet day. The phenomenon is termed as the

[1]Department of Physics, Raja Peary Mohan College, Uttarpara, India.
[2]Indian Institute of Geomagnetism, Navi Mumbai, India.

Corresponding author: S. K. Chakraborty, Department of Physics, Raja Peary Mohan College, Uttarpara 712258, India. (skchak2003@yahoo.com)

0148-0227/12/2012JA017808

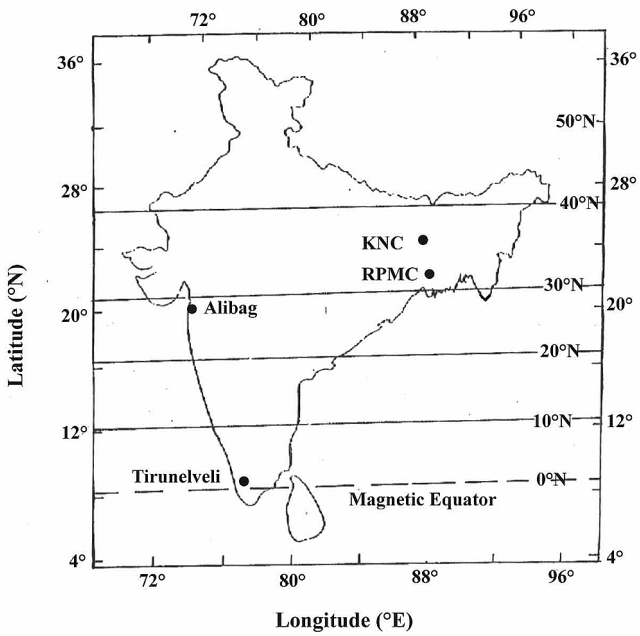

Figure 1. Location of the observing stations KNC (VHF and GPS), RPMC (VHF), Alibag/ABG (magnetometer) and Tirunelveli/TIR (magnetometer and ionosonde). Geographic latitudes and longitudes are shown. Horizontal lines indicate isodip lines (geomagnetic).

CEJ event and is manifested by depression of H below its nighttime level [*Gouin*, 1962; *Gouin and Mayaud*, 1967].

[5] As EEJ represents intensification of equatorial electric field, a good correspondence is noted between EEJ strength and daytime $\boldsymbol{E} \times \boldsymbol{B}$ vertical plasma drift at the magnetic equator [*Anderson et al.*, 2002]. During normal EEJ days, there is a high degree of correlation between the strength of EIA and day's EEJ strength [*Sethia et al.*, 1980] or time-integrated EEJ throughout the day [*Raghavarao et al.*, 1978; *Rama Rao et al.*, 2006; *Chakraborty and Hajra*, 2009]. While normal EEJ facilitates the development of EIA, CEJ adversely affects it. The weakening or disappearance of fountain effect leading to perturbation in EIA during afternoon hours on CEJ days was reported by numerous studies [*Rajaram and Rastogi*, 1974; *Deshpande et al.*, 1977; *Chandra et al.*, 1979; *Hajra et al.*, 2009]. Also, a close linkage between the well-developed EIA and postsunset irregularities is unambiguously established by ground-based ionospheric observations, and is being attempted to be utilized in developing predictive capability of the irregularities during last two decades [*Raghavarao et al.*, 1988; *Sridharan et al.*, 1994; *Valladares et al.*, 2001; *Thampi et al.*, 2006; *Chakraborty et al.*, 2012]. Variability of afternoon EIA and triggering of postsunset irregularities are controlled mainly by postsunset prereversal enhancement (PRE) of eastward electric field. Recently *Prakash et al.* [2009], using numerical simulation technique, suggested a feedback mechanism between fairly strong EIA around 1700 LT (local time) and PRE. *Kelley et al.* [2009] suggested that normal PRE results from the closure of EEJ through the postsunset *F* region [*Haerendel and Eccles*, 1992]. An appreciable number of studies reported association between daytime EEJ and PRE of vertical drift. The abnormal height rise of the postsunset equatorial F-layer followed by intense equatorial spread-F (ESF) was attributed [*Sastri*, 1998] to the enhanced daytime EEJ even during low solar activity periods. *Dabas et al.* [2003] reported good correlations of day's EEJ strength with some parameters like h′F (F-layer virtual height), $\boldsymbol{E} \times \boldsymbol{B}$ drift around 1800 LT and magnitude of postsunset secondary maximum in total electron content (TEC) around low latitude region. It was suggested that day's EEJ strength might be a very useful parameter for prediction of equatorial plasma bubbles and associated irregularities. The positive contributions of daytime EEJ parameters to the postsunset *F* region electrodynamics favorable for generation of irregularities are also supported by recent studies [*Sreeja et al.*, 2009; *Uemoto et al.*, 2010]. Present paper deals with some case studies involving ESF and scintillation events in the context of variation of EEJ. It will be found that EEJ strength that is determined by noontime peak value may not effectively dictate the postsunset phenomena, i.e., day-to-day variability of the postsunset density irregularities may not be simply interpreted in terms of noontime EEJ variation. Contrary to the normal EEJ conditions, contributions of equatorial electrodynamics on the evolution of equatorial irregularities on the days of CEJ events are yet to be explored. According to *Bhargava and Sastri* [1977], on the CEJ days an additional semidiurnal current is superposed on the normal EEJ current, which is reflected in a northward peak at prenoon hours followed by an afternoon time southward peak in the variation of geomagnetic H field at the magnetic equator. It should have modulating effects on the afternoon as well as evening time electrodynamics over the magnetic equator. It is interesting to study the effects of afternoon CEJ events on the ambient conditions for evolutions of ionization anomaly and postsunset density irregularities. No significant study on this aspect is reported till date. Under present investigation multitechnique case studies are made to assess the contributions of varied equatorial electrodynamics under normal and counter electrojet conditions to the day-to-day variabilities of postsunset evolution of plasma density irregularities leading to ESF and scintillation.

2. Data and Method of Analysis

[6] The present investigation attempts to describe multitechnique studies on the variabilities of the ambient ionization and evolution of postsunset irregularities under varying electrodynamical conditions of normal EEJ and CEJ events. VHF (250 MHz) amplitude scintillation data from two observing stations, Raja Peary Mohan College (RPMC), Hooghly (geographic lat: 22.65°N, long: 88.36°E, dip: 33.6°N) and Krishnath College (KNC), Berhampore (geographic lat: 24.09°N, long: 88.25°E, dip: 36.35°N) are utilized in the study (Figure 1). The observing stations are situated around the EIA crest, more or less along the same meridian. The region is considered to be most sensitive to exhibit effects related to equatorial electrodynamics. The VHF data are recorded digitally at a sampling rate of 20 Hz.

[7] A dual frequency GPS receiver is installed at KNC to record the scintillations at L1 (1575.42 MHz) frequency along with total electron content (TEC) data at an interval of 1 min. An elevation cut-off of 10° is selected to avoid multipath effect.

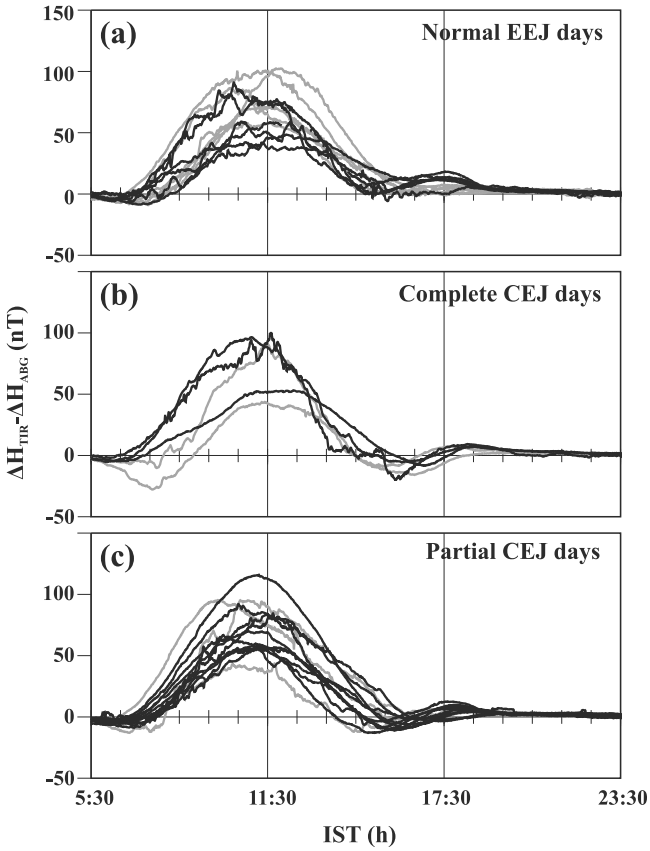

Figure 2. Diurnal variations of EEJ during (a) normal EEJ, (b) complete CEJ and (c) partial CEJ days for the period from 25 March to 25 April 2011. The black and gray curves pertain to days with and without postsunset ESF events.

[8] To have an approximate idea of EIA development, global ionospheric maps (GIMs) of vertical TEC are also analyzed. GIM TEC data at a temporal resolution of 15 min and spatial resolution of 5° × 2.5° in geographic longitude × latitude are obtained from the Website of International GNSS Service Working Group, NASA (http://igscb.jpl.nasa.gov/).

[9] For information regarding ESF which is a signature of density irregularities of various scale sizes, variations of the virtual height of F-layer (h′F) and F_2-layer critical frequency (f_oF_2), ionograms at 10 min interval at the equatorial station Tirunelveli (geographic lat: 8.73°N, long: 77.70°E, dip: 0.6°N) are analyzed.

[10] Data on geomagnetic field horizontal (H) components at 1 min resolution are collected with magnetometers located at Tirunelveli (TIR) (geographic lat: 8.73°N, long: 77.70°E, dip: 0.6°N) and Alibag (ABG) (geographic lat: 18.63°N, long: 72.87°E, dip: 23°N). Following the method suggested by *MacDougall* [1969] and *Chandra and Rastogi* [1974], the hourly variations of H relative to its nighttime values at Alibag (ΔH_{ABG}) are subtracted from the corresponding values at Tirunelveli (ΔH_{TIR}) to estimate the EEJ strength, ΔH_{TIR}-ΔH_{ABG}. Tirunelveli is an EEJ station while Alibag is located outside the EEJ belt (Figure 1). On CEJ days, the difference field (ΔH_{TIR}-ΔH_{ABG}) shows negative values during afternoon hours. *Rastogi* [1974] reported some events when the H field near the magnetic equator (ΔH_{TIR}) does not fall below the nighttime level, but the difference field (ΔH_{TIR}-ΔH_{ABG}) exhibits negative values. These are termed as partial CEJ events. The days of observations are separated on the basis of normal EEJ, complete and partial CEJ days. It may be mentioned that the VHF/GPS stations and ionosonde/magnetometer stations are not situated along the same meridian (Figure 1). There is a longitude difference (∼10°) large enough for point-to-point correspondence but the average picture may be assumed to be the same.

[11] Simultaneous availability of magnetometer, ionosonde, VHF/GPS measurements restricts the period of observations from 25 March to 25 April 2011 of the vernal equinoctial months. During the period $F_{10.7}$ solar flux varies in the range of 105–130 solar flux units (10^{-22} W m^{-2} Hz^{-1}). Only the days with $D_{st} > -50$ nT, i.e., geomagnetically quiet days [*Akasofu*, 1981] are considered for the present investigation.

3. Results

[12] Figure 2 shows the mass plots of diurnal variations of EEJ for days with (Figure 2a) normal EEJ, (Figure 2b) complete afternoon CEJ events and (Figure 2c) partial afternoon CEJ events respectively during the period of observation. All the days are geomagnetically quiet. The black and gray curves pertain to the days with and without postsunset ESF events respectively.

[13] In Figure 2a it may be noted that there are two normal EEJ days when the diurnal peak values are remarkably high (∼100 nT) and occurs at comparatively later local time (around 1200 IST) (IST, Indian standard time = universal time (UT) + 0530 h) than the others. On these days no signature of postsunset irregularities is recorded at equatorial and low latitude zone. In fact a detailed analysis of the diurnal EEJ variations during normal EEJ, complete and partial CEJ days is unable to detect any parameter of daytime EEJ, like daytime peak value, its occurrence time, time-integrated value throughout the day and prenoon developing/afternoon decaying slope, that may consistently dictate the day-to-day occurrence/non-occurrence of postsunset irregularities. The result deviates from the previously reported statistical results [*Dabas et al.*, 2003; *Sreeja et al.*, 2009] suggesting prediction of postsunset irregularities employing noontime peak EEJ/prenoon EEJ variation. A significant difference may, however, be noted in EEJ variations after ∼1600 IST between days with and without postsunset ESF. In all three cases, the EEJ values around the period seem to be somewhat enhanced on the days with postsunset ESF.

[14] The numbers of normal EEJ, complete and partial CEJ days during the period of observation are 12, 5 and 13 respectively. The days exhibiting postsunset irregularity phenomena (ESF) are respectively 6, 3 and 10. Postsunset irregularities seem to occur preferentially on the days with afternoon partial CEJ event. The days are found to be characterized by intensification of EEJ around the sunset hours. It may be mentioned that at Tirunelveli, postsunset ESF is recorded on 19 days while postsunset VHF scintillation at RPMC/KNC is observed for 10 days. All the scintillation events are preceded by ESF at Tirunelveli. Scintillation is caused by irregularities of specific scale sizes. The evolution, dynamics, lifetime of irregularities of various scale sizes in addition to longitude difference between ESF and scintillation monitoring stations restrict the point-to-point

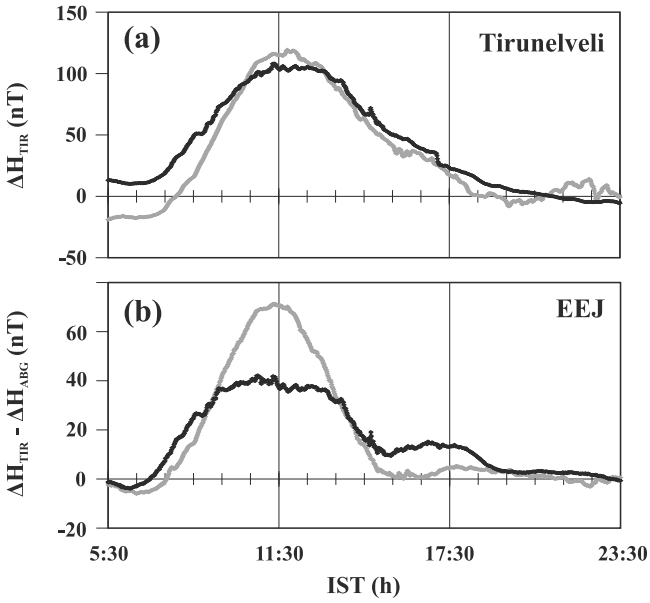

Figure 3. Diurnal variations of (a) horizontal component of geomagnetic field relative to its nighttime values (ΔH) at Tirunelvelli and (b) EEJ on the day with postsunset ESF, 31 March 2011 (black curve) and the non-ESF day, 11 April 2011 (gray curve).

correspondence between the two phenomena. To investigate distinguishing features between days with and without postsunset irregularities, detailed case studies are conducted under varying electrodynamical conditions leading to occurrence/non-occurrence of postsunset irregularities in the equatorial and low latitude zone.

3.1. Normal Electrojet Days

[15] The diurnal variations of horizontal component (H) of geomagnetic field at the equatorial station Tirunelvelli along with the estimated EEJ in the Indian zone during an ESF day (31 March 2011) and a non-ESF day (11 April 2011) are shown in Figure 3. For the equatorial station (Tirunelvelli), daytime peak value is somewhat larger on 11 April than on 31 March though the reverse is true for afternoon values (Figure 3a). Prominent differences may, however, be noted in the EEJ variations between the two days (Figure 3b). On 11 April, the EEJ increases sharply from about 0630 IST to attain a diurnal peak of ∼70 nT around 1130 IST, followed by sharp decreasing trend till 1530 IST. EEJ thereafter approaches nighttime level with some fluctuations. On the other hand, the prenoon increase as well as afternoon decay rates of EEJ on 31 March are much more slow and a "flattop" nature is observed around 0930–1300 IST with peak value of ∼40 nT around 1100 IST. Most interestingly, a secondary enhancement is recorded after 1530 IST which reaches peak value ∼15 nT around 1630 IST. Also, significantly high value of EEJ persists till 1900 IST, implying intensification of EEJ field around sunset hours on 31 March compared to that on 11 April.

[16] Ionograms at the equatorial station Tirunelvelli are analyzed to study the differential effects, if any, on the equatorial *F* region behavior. Figure 4 shows the variations of $h'F$ and f_oF_2 during afternoon-to-premidnight sector. On 11 April, $h'F$ reaches a peak value of 330 km around 1930 IST and maximum vertical drift velocity, which may be considered to be an index of PRE electric field, is estimated to be ∼9 m/s. A much sharper increase in $h'F$ leading to much higher F-layer altitude (peak $h'F$ > 380 km) and consequent higher drift velocity (∼25 m/s) are noted on 31 March. Also, f_oF_2 at the equatorial station is found to decrease significantly after 1530 IST on 31 March compared to that on 11 April. The decreasing trend in f_oF_2 at the equatorial station may indicate resurgence of EIA around sunset hours on 31 March. The measurements of $h'F$ and f_oF_2 are disturbed after 1910 IST due to evolution of ESF (range spread-F). The variations of $h'F$ and f_oF_2 at the equatorial station indicate strengthening of eastward equatorial electric field responsible for F-layer vertical drift and consequent generation of postsunset irregularities on 31 March.

[17] To have an approximate idea of EIA variations, GIM TEC data along 90°E longitude zone are analyzed (Figure 5). As observed from the contour plots, the development of EIA is delayed till about 1100 IST on 31 March compared to 11 April when EIA starts to develop from 0900 IST. It may be related to the weaker prenoon development of EEJ on 31 March than on 11 April (Figure 3b). In spite of this difference, on both the days anomaly develops most strongly with peak crest values of ∼75–80 TECU (TEC unit, 10^{16} electrons/m^2) around 1400–1500 IST. The time follows a delay of ∼2.5–3 h after the peak development of EEJ (Figure 3b). During this period the northern peak is situated around 10–15°N magnetic latitude while southern peak around 15–20°S magnetic latitude. The anomaly

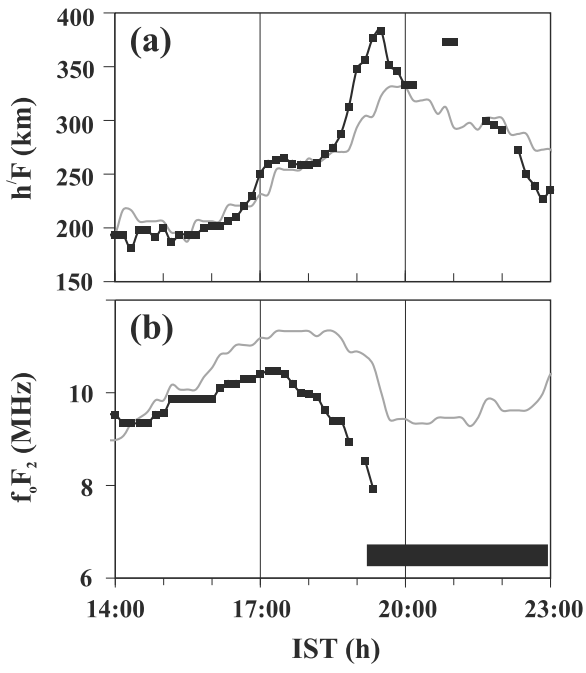

Figure 4. Variations of (a) $h'F$ and (b) f_oF_2 at the equatorial station Tirunelvelli during local afternoon-premidnight sector. The filled squares connected with black curve pertain to 31 March 2011 while gray curve to 11 April 2011. On 31 March the measurements of $h'F$ and f_oF_2 are disrupted after 1910 IST due to presence of ESF. The time period of ESF is indicated by horizontal bar in the lower panel.

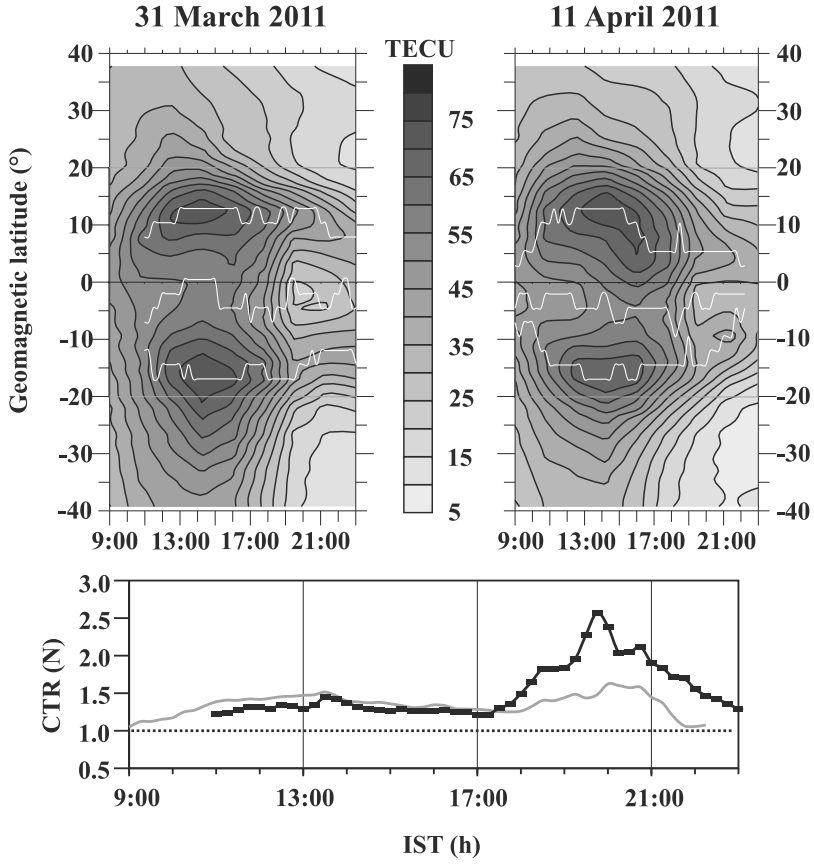

Figure 5. (top) Contour plots showing variations of GIM TEC with geomagnetic latitude and time (IST h) along 90°E geographic longitude on 31 March 2011 and 11 April 2011. The white curves embedded on the contours present temporal variations of geomagnetic latitudes of the northern crest, trough and southern crest of EIA respectively. (bottom) Diurnal variations of northern crest-to-trough ratio (CTR (N)) along 90°E geographic longitude on 31 March (filled squares connected with black curve) and 11 April (gray curve). The discontinuity in the curves implies absence of anomaly structure.

strength decreases significantly after about 1700 IST that may correspond to the afternoon minimum of EEJ around 1530 IST. After 1700 IST, the EIA structures are found to register distinctive features between the two days. The crests are weak, converging and asymmetrically distributed (~5°N and 12°S) around the magnetic equator on 11 April. On the contrary, strong, wide spread and more or less latitudinally symmetric (~12°N, 14°S) anomaly is found to persist throughout the postsunset hours on 31 March. To have a more lucid picture, diurnal variations of northern crest-to-trough ratios (CTR (N)) estimated from the GIM TEC are considered for the two days (Figure 5, bottom). CTR may be taken as a measure of strength of the anomaly. Interestingly, on 31 March, the CTR increases drastically after 1700 IST and reaches peak value around 2000 IST. It confirms the resurgence of strong (in terms of crest-trough formation) anomaly structure on 31 March throughout the postsunset sector, which is not true for 11 April. The resurgence of anomaly may be instigated by the strong eastward electric field over the magnetic equator that is reflected in the enhanced F-layer height rise and/or drift velocity (Figure 4a) preceded by secondary enhancement in EEJ (Figure 3b) on 31 March.

[18] Consistent with (1) the electrodynamical conditions prevailing near the magnetic equator and (2) ambient ionization distribution around the low latitude zone, VHF amplitude scintillations are recorded from the two observing stations RPMC and KNC during postsunset hours of 31 March, while no signature of scintillation is recorded on 11 April (Figure 6). It may be noted that scintillation patches at RPMC initiate earlier, persist for longer duration with higher intensity (S_4) than those at KNC. The features are consistently the same throughout the period of observations. It may signify that the irregularities generated near the magnetic equator are mostly responsible for scintillation around the stations.

[19] The evolution of the equatorial irregularity phenomena during the postsunset hours of 31 March in the low latitude zone may be more evident from Figure 7 where various GPS satellite tracks (ionospheric piercing point (IPP)) at 1 h interval are shown. The durations and positions of tracks exhibiting scintillations at L1 frequency are marked by large circles. It may be mentioned that initiation of spread-F irregularities at the equatorial station Tirunelveli (8.73°N, 77.7°E) occurs around 1910 IST (Figure 4). VHF scintillations are recorded to initiate at ~2009 IST at RPMC

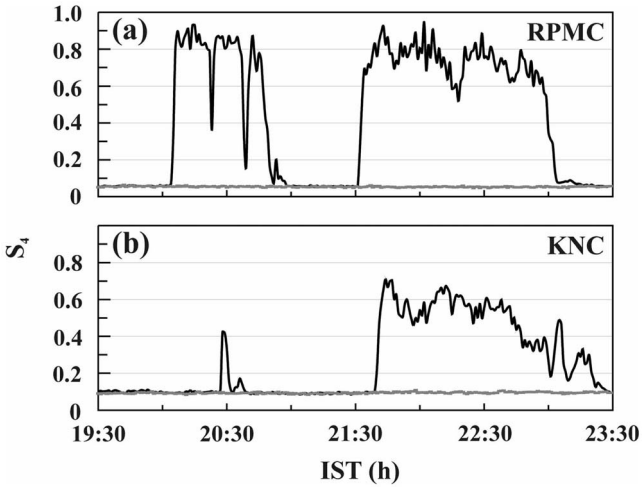

Figure 6. Temporal variations of S_4 index at VHF (250 MHz) at (a) RPMC and (b) KNC during the postsunset hours of 31 March 2011 (black curve) and 11 April 2011 (gray curve).

(22.65°N, 88.36°E) and at ~2027 IST at KNC (24.09°N, 88.25°E) (Figure 6). The signature of the scintillation at L1 frequency is recorded in the track of PRN#11 at earlier time (1950 IST) when the corresponding IPP passed through the geographic location of (18.07°N, 90.87°E). Scintillation thereafter plagued the low latitude region around the anomaly crest as is evident from the temporal hierarchy of Figures 7a–7d. This is consistent with the equatorial origin and dynamics of the irregularities. Scintillation events on the GPS tracks are mostly associated with TEC depletions/bite-outs indicating plasma bubble induced irregularities.

[20] All the observations presented above establish the strengthening of eastward electric field at the magnetic equator in association with enhanced EEJ variation after ~1600 IST during normal EEJ days. The eastward electric field modulates ionization distribution in the low latitude zone and facilitates the evolution of equatorial irregularities in the postsunset hours.

[21] It should be mentioned that around 2000–2100 IST (Figure 7b) scintillation is detected on the track of PRN#6 around 30°N–95°E zone. Irregularities generated at the eastern longitude sector of the VHF stations, depending on the apex altitude reached, may produce scintillation. Owing to unavailability of any GPS track on south of the region temporal evolution of scintillation in this region cannot be tracked.

3.2. Counter Electrojet Days

[22] Diurnal variations of geomagnetic field H component at the equatorial station Tirunelveli along with the estimated EEJ from the Indian zone on three CEJ days, 26 March, 19 April and 23 April 2011 are plotted in first two panels of Figures 8a and 8b. Though the EEJ variations register

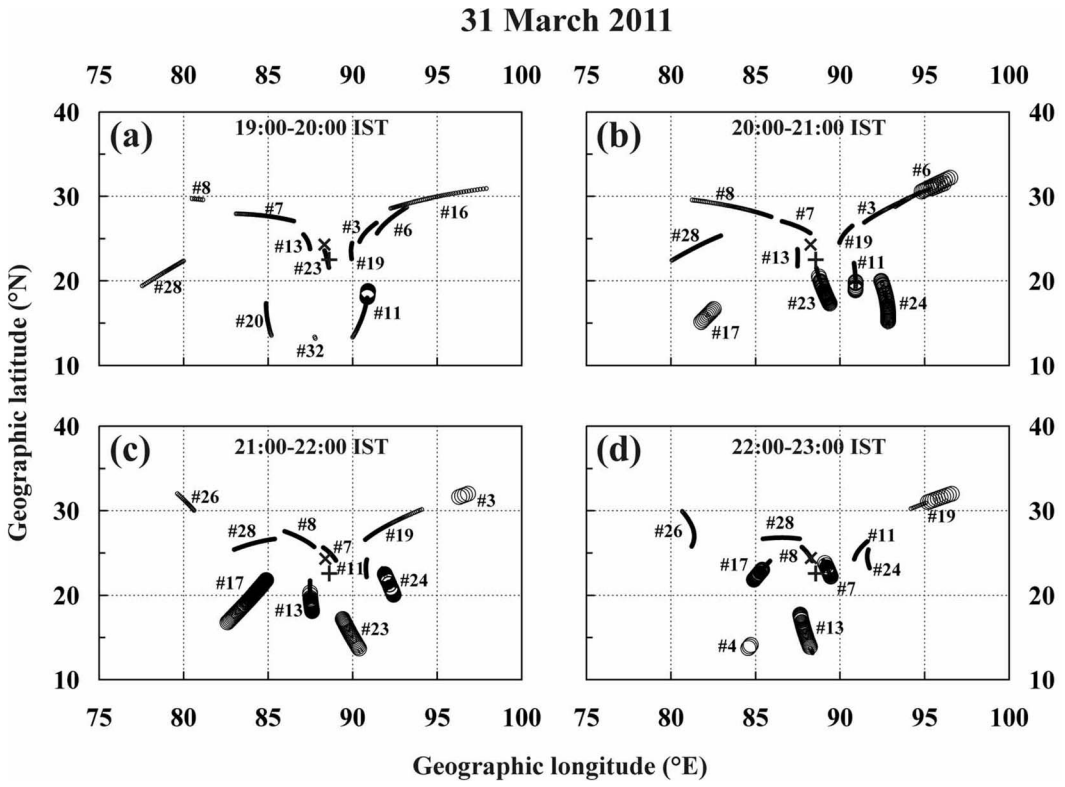

Figure 7. Latitude-longitude (geographic) plots of the ionospheric pierce points (IPPs) of the GPS satellite tracks observed from KNC during postsunset hours (1900–2300 IST) on 31 March 2011. The tracks exhibiting scintillations at L1 frequency are marked by large circles. Temporal evolution feature of the irregularities is evident in the plots. In each plot the 'plus' and 'cross' marks represent the locations of RPMC and KNC respectively.

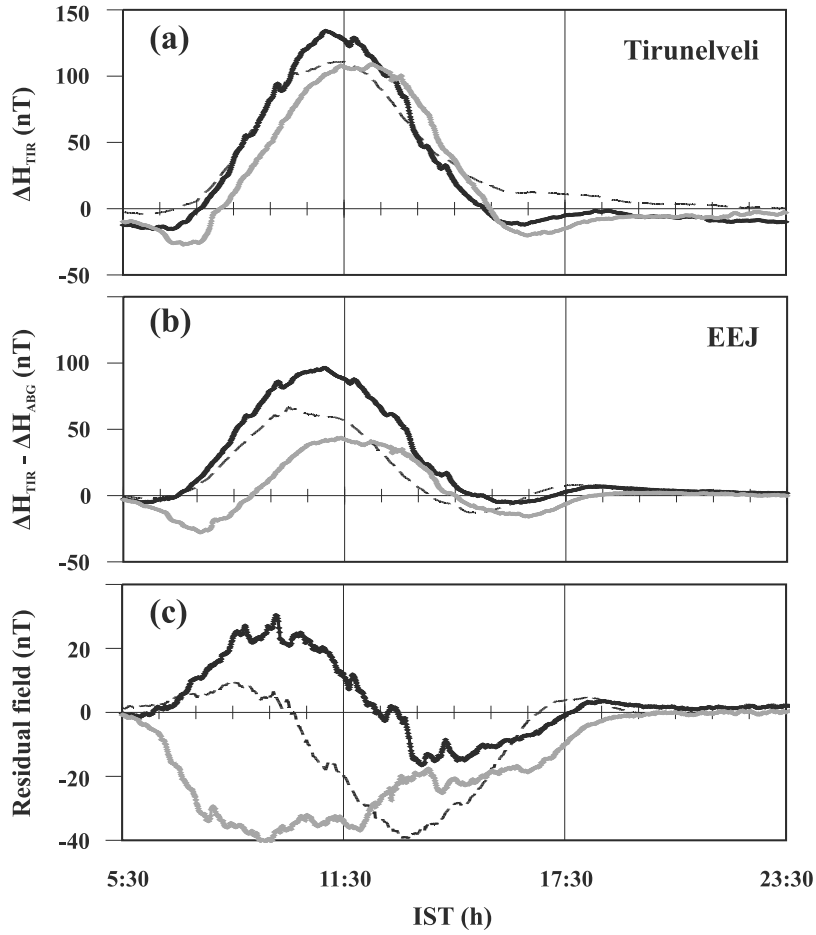

Figure 8. Diurnal variations of (a) horizontal component of geomagnetic field relative to its nighttime values (ΔH) at Tirunelveli, (b) EEJ and (c) residual field (see text for definition) on 26 March 2011 (dotted curve), 19 April 2011 (black curve) and 23 April 2011 (gray curve). 26 March is a partial CEJ day while 19 April and 23 April are complete CEJ days. Postsunset ESF is recorded on 26 March and 19 April while no such event is recorded on 23 April.

afternoon negative values on all three days (Figure 8b), on 26 March the H field at the equatorial station (Tirunelveli) never decreases below the nighttime level (Figure 8a) indicating partial CEJ event. While postsunset ESF is recorded on 26 March and 19 April, no such event is noted on 23 April. It should be mentioned that the peak value in EEJ on 23 April is found to be comparable to that on 26 March and EEJ attains peak value at later time on 23 April than on other two days. According to *Bhargava and Sastri* [1977], on the days of afternoon CEJ events a field of semidiurnal nature, presumably due to the CEJ, is superposed on the normal quiet day electrojet field. Considering the hypothesis, a reference field is estimated using normal EEJ days of the observation period. The diurnal reference variations are subtracted from the diurnal EEJ variations during the three CEJ days. The resultant residual fields which may be considered to be related solely to CEJ are plotted in Figure 8c. On 26 March and 19 April, a prenoon eastward field is found to be followed by a westward field, while there is no signature of eastward field during prenoon/noon period on 23 April. Another interesting difference may be noted during sunset hours. On 26 March and 19 April, the residual field is eastward and significantly enhanced, while the residual field is much lower and there is no signature of eastward field during the period on 23 April.

[23] The differences in equatorial electric field variations around the sunset time are also reflected in the variations of equatorial F-layer parameters (Figure 9). After about 1800 IST, h$'$F increases abruptly on 26 March and 19 April attaining peak heights of ~387 km and 402 km respectively. The peak drift velocities are estimated to be ~21 m/s and 24 m/s respectively. On the contrary, a significantly lower drift velocity (~7 m/s) and a comparatively lower height rise (~275 km) are recorded on 23 April. The observations confirm the existence of strong eastward electric field around the sunset hours on 26 March and 19 April. Following these electrodynamical conditions, while strong ESF (range spread-F) are recorded from 1930 IST on these days, no such irregularity phenomenon is noted on 23 April. Also, due to strong eastward electric field around local sunset hours on 26 March and 19 April, a decreasing trend is reflected in f_oF_2 at the equator on these days indicating transport of equatorial ionization to the off-equatorial locations and evening resurgence of EIA.

[24] The diurnal evolutions of the anomaly structure on these days are evident in the GIM TEC plots along 90°E

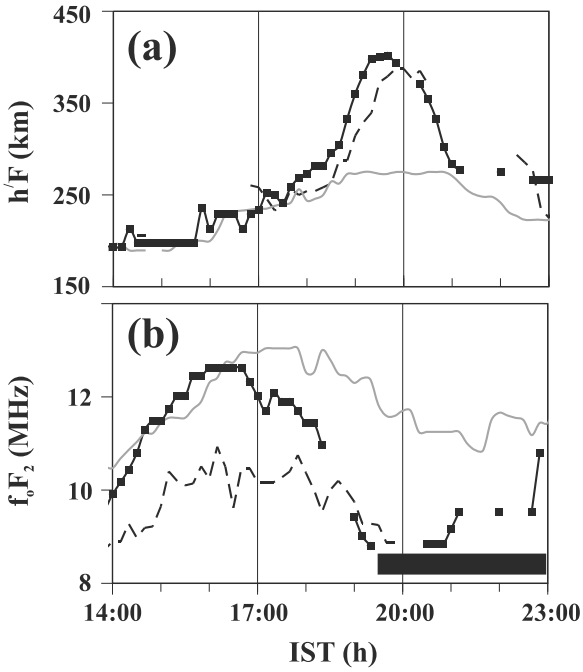

Figure 9. Variations of (a) h′F and (b) f_oF_2 at the equatorial station Tirunelveli during afternoon-premidnight sector on 26 March 2011 (dotted curve), 19 April 2011 (filled squares connected with black curve) and 23 April 2011 (gray curve). The horizontal bar in the lower panel indicates the time period of ESF on 26 March and 19 April.

meridian (Figure 10). Consistent with the highest EEJ peak value (Figure 8b), the noontime EIA develops most strongly on 19 April. Due to morning CEJ event on 23 April, the development of EIA/crest-trough formation is delayed till ~1000 IST. EIA weakens drastically around 1630 IST and seems to disappear after ~1700 IST on this day. On the contrary, conspicuous secondary developments of EIA after 1800 IST are recorded on the other two days (26 March and 19 April) which are much more clear in the CTR plots of Figure 10 (bottom). All the features result from the strong afternoon electric field over the magnetic equator, as revealed through EEJ variations (Figure 8b) and reflected in h′F variations (Figure 9a).

[25] VHF scintillations at RPMC and KNC as well as scintillations at GPS L1 frequency (not shown) are recorded in the low latitude zone during postsunset hours of 26 March and 19 April while no such events are recorded on 23 April.

[26] Clearly, on the days of afternoon CEJ events, complete or partial, strengthening of equatorial eastward electric field as revealed in the variation of h′F or drift velocity is found to be associated with the enhanced residual field after ~1700 IST. It seems to trigger hierarchy of equatorial electrodynamics related phenomena, reflected in the measurements of VHF, GIM TEC and GPS observations.

4. Discussion

[27] The Rayleigh-Taylor (R-T) instability is widely accepted as the basic mechanism responsible for the generation of equatorial irregularities [*Ossakow*, 1981; *Sultan*, 1996; *Abdu et al.*, 2009] (G. Haerendel, Theory of equatorial spread F, unpublished report, Max-Planck-Institut für Physik und Astrophysik, Garching, Germany, 1973). The instability is considered to be triggered at the bottomside F-layer, where a steep density gradient develops after sunset due to the combined effects of (1) the PRE in the vertical plasma drift over the magnetic equator and (2) the fast chemical recombination of the dominant molecular ions in the absence of production by solar ionizing radiation. The primary requisites for the triggering of irregularities are the vertical drift of F-layer to the region of low collision frequency, and appearance of a seed perturbation at the altitude of the steep density gradient. However, *Abdu* [2001] asserted that the vertical drift alone is not sufficient to describe the onsets of density irregularities. The neutral winds – both zonal and meridional components which introduce changes in the field line-integrated Pedersen conductivity – are also important factors [*Maruyama and Matuura*, 1984; *Maruyama*, 1988; *Mendillo et al.*, 1992; *Saito and Maruyama*, 2006]. In fact, varied combinations of background electron density gradient, F-layer vertical drift velocity, neutral wind system are expected to play dominant role in the day-to-day variability of irregularities which is considered to be the most enigmatic aspect of the modern ionospheric physics.

[28] In the present paper, comprehensive case studies on the day-to-day variations of ambient ionization and equatorial irregularities under varying electrodynamical conditions of normal EEJ, complete and partial CEJ events during vernal equinox of 2011 are presented from Indian equatorial and low latitude zone. The period of observation is characterized by large variability in the equatorial electrodynamics as revealed through the diurnal variations of geomagnetic field at the magnetic equator as well as EEJ. On normal EEJ days, large day-to-day variability is recorded during daytime as well as around sunset hours. The noontime EEJ is found to be not so efficient to dictate the day-to-day variabilities of postsunset EIA and evolution/inhibition of equatorial irregularities. The ESF days are, however, found to be characterized by the secondary enhancements in EEJ after ~1530 IST followed by sustenance of high values till 1900 IST compared to the non-ESF days. Thus the variation of EEJ after 1530 IST, not during noontime hours, seems to play the dominant role in dictating the postsunset resurgence of EIA and triggering of irregularities. The variations of h′F and vertical drift velocities at the magnetic equator are the signatures of the postsunset strengthening of eastward equatorial electric field on the days with enhanced EEJ after ~1530 IST.

[29] On the days with complete and partial afternoon CEJ events, the equatorial electrodynamics is largely modified throughout the day and evening hours. In general, as on normal EEJ days, the CEJ days with postsunset resurgence of EIA and subsequent generation of irregularities are characterized by enhanced values of EEJ after ~1600 IST compared to days without postsunset irregularities. The residual fields presumably due to CEJ events are also found to exhibit distinguishing features. The nights with well-developed EIA and postsunset irregularities are found to be preceded by well-structured residual fields with prenoon eastward component, noontime westward component followed by significantly enhanced eastward component during sunset hours. On the other hand, westward residual field throughout the day and weakening of the field around sunset hours leading

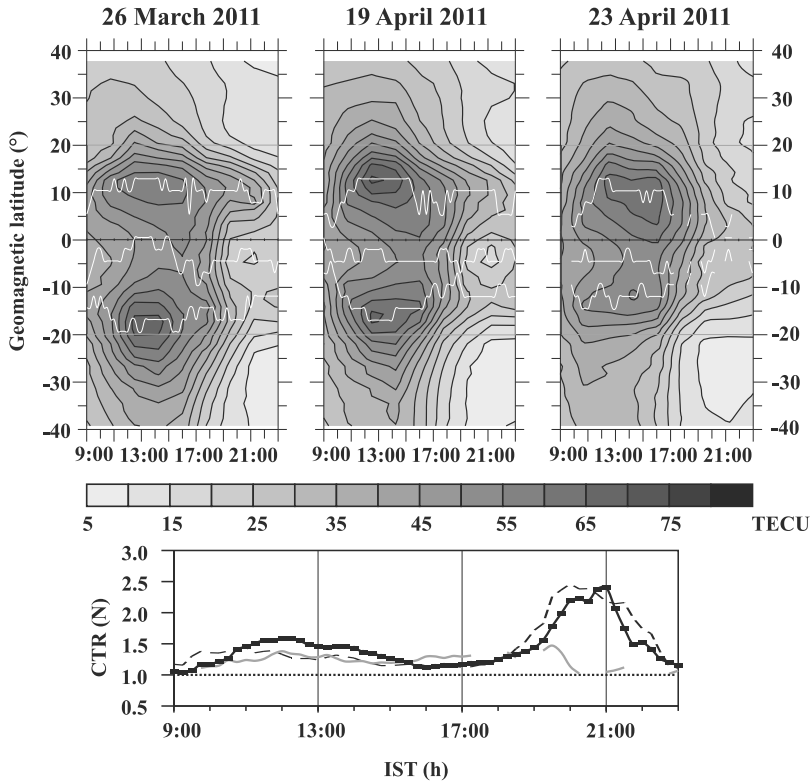

Figure 10. (top) Contour plots showing variations of GIM TEC with geomagnetic latitude and time (h IST) along 90°E geographic longitude on 26 March 2011, 19 April 2011 and 23 April 2011. The white curves embedded on the contours present temporal variations of geomagnetic latitudes of the northern crest, trough and southern crest of EIA respectively. (bottom) Diurnal variations of northern crest-to-trough ratio (CTR (N)) along 90°E geographic longitude on 26 March (dotted curve), 19 April (filled squares connected with black curve) and 23 April (gray curve). The discontinuity in the curves implies absence of anomaly structure.

to inhibition of anomaly structure characterize the non-ESF day. The enhanced residual fields during sunset hours are suggested to be the indications of strong eastward electric field during the period, as evident in the variations of F-layer height rise and drift velocity at the magnetic equator.

[30] The present study reveals the importance of variability of EEJ after ∼1600 IST in the context of resurgence of EIA and triggering of postsunset irregularities. As mentioned earlier, the variabilities of the postsunset ionospheric phenomena during geomagnetically quiet days are primarily dependent on the variations of PRE of eastward electric field before its reversal to the westward direction. Though PRE is primarily attributed to the *F* region dynamo that becomes dominant at sunset when the *E* region conductivity decreases abruptly, control of EEJ on PRE is suggested by earlier studies [e.g., *Balsley and Woodman*, 1969; *Haerendel and Eccles*, 1992; *Kelley et al.*, 2009; *Su et al.*, 2009]. *Balsley and Woodman* [1969] reported simultaneous enhancements in *E* region westward and *F* region upward drift velocities, both of which are proportional to the eastward electric field, confirming experimentally the EEJ control on the postsunset F-layer drift. Under present investigation larger F-layer base heights and/or enhanced F-layer drift velocities are observed in association with enhanced values of EEJ around sunset hours. Continuation of EEJ in the postsunset ionosphere after 1800 LT is attributed to the sustenance of finite conductivity across the sunset terminator [*Hari et al.*, 1996; *Su et al.*, 2009]. It was suggested that the observation of EEJ after 1800 LT can be used as a reference for the variation of the postsunset *F* region plasma drift. The *F* region zonal electric field during postsunset hours is reported to be contributed by both F- and E- region dynamo actions [*Hari et al.*, 1996; *Su et al.*, 2009]. Model study by *Farley et al.* [1986] suggested that the contributions of *E* region dynamo to the day-to-day, seasonal and solar cycle changes in the PRE can be comparable to those of *F* region. Owing to the current continuity requirement from evening *F* region dynamo, EEJ flows in a low conducting *E* region around sunset and a vertical divergent current of EEJ connects the vertical *F* region dynamo current [*Haerendel and Eccles*, 1992]. Secondary enhancements in EEJ after ∼1530 IST on normal EEJ days and significantly enhanced residual fields after ∼1700 IST on complete and partial CEJ days – as revealed in the present study – may strengthen the normal PRE electric field and consequently facilitate the resurgence of EIA and evolution of postsunset density irregularities.

5. Summary

[31] The present paper deals with the evolution of postsunset irregularities under varying electrodynamical conditions during vernal equinoctial months (March–April) of

2011. Multitechnique case studies from Indian equatorial zone involve simultaneous measurements using magnetometers, ionosonde, VHF and GPS receivers.

[32] On the days of normal EEJ as well as complete and partial CEJ events, the electrodynamical conditions as revealed through the EEJ variations around the noontime period may not consistently dictate the day-to-day variability of postsunset equatorial irregularities.

[33] On the contrary, afternoon/evening time variation of eastward electric field as revealed through EEJ seems to play dominant role in dictating postsunset resurgence of EIA and consequent generation of spread-F irregularities in the low latitude zone on the normal EEJ days.

[34] On complete and partial CEJ days, residual fields presumably due to the events are found to register distinct features between days with and without postsunset irregularities. The nights with well-developed EIA, postsunset spread-F near the magnetic equator and consequent irregularity phenomena around the low latitude zone are found to be preceded by well-structured residual fields with prenoon eastward component, noontime westward component followed by significantly enhanced eastward component during sunset hours. A westward residual field throughout the day and/or weakening of the field around the sunset hours may perturb the anomaly structure and inhibit the irregularity phenomena.

[35] It may be mentioned that the accrued results are based on a few case studies during vernal equinoctial months. More case as well as statistical studies under varying geophysical conditions are required for development of predictive capability or model.

[36] **Acknowledgments.** The authors are indebted to Ashish DasGupta, University of Calcutta, for valuable discussions. The authors wish to thank Diwakar Tiwari, IIG, Mumbai, for supplying ionosonde data. One of the authors (R.H.) is thankful to ISRO for research fellowship through RESPOND program. The work has been carried out with the financial assistance of DST, Government of India.

[37] Robert Lysak thanks James Whalen and another reviewer for their assistance in evaluating the paper.

References

Abdu, M. A. (2001), Outstanding problems in the equatorial ionosphere-thermosphere electrodynamics relevant to spread F, *J. Atmos. Sol. Terr. Phys.*, *63*, 869–884, doi:10.1016/S1364-6826(00)00201-7.

Abdu, M. A., I. S. Batista, B. W. Reinisch, J. R. Souza, J. H. A. Sobral, T. R. Pedersen, A. F. Medeiros, N. J. Schuch, E. R. de Paula, and K. M. Groves (2009), Conjugate point equatorial experiment (COPEX) campaign in Brazil: Electrodynamics highlights on spread F development conditions and day-to-day variability, *J. Geophys. Res.*, *114*, A04308, doi:10.1029/2008JA013749.

Akasofu, S.-I. (1981), Relationships between the AE and D_{st} indices during geomagnetic storms, *J. Geophys. Res.*, *86*, 4820–4822, doi:10.1029/JA086iA06p04820.

Anderson, D., A. Anghel, K. Yumoto, M. Ishitsuka, and E. Kudeki (2002), Estimating daytime vertical $\boldsymbol{E} \times \boldsymbol{B}$ drift velocities in the equatorial *F* region using ground-based magnetometer observations, *Geophys. Res. Lett.*, *29*(12), 1596, doi:10.1029/2001GL014562.

Appleton, E. V. (1946), Two anomalies in the ionosphere, *Nature*, *157*, 691–693, doi:10.1038/157691a0.

Balsley, B. B., and R. F. Woodman (1969), On the control of the *F* region drift velocity by the *E* region electric field: Experimental evidence, *J. Atmos. Terr. Phys.*, *31*, 865–867, doi:10.1016/0021-9169(69)90167-6.

Basu, S., K. M. Groves, S. Basu, and P. J. Sultan (2002), Specification and forecasting of scintillations in communication/navigation links: Current status and future plans, *J. Atmos. Sol. Terr. Phys.*, *64*, 1745–1754, doi:10.1016/S1364-6826(02)00124-4.

Bhargava, B. N., and N. S. Sastri (1977), A comparison of days with and without occurrence of counter-electrojet afternoon events in the Indian region, *Ann. Geophys.*, *33*, 329–333.

Booker, H., and H. W. Wells (1938), Scattering of radio waves by the F region of the ionosphere, *J. Geophys. Res.*, *43*, 249–256, doi:10.1029/TE043i003p00249.

Chakraborty, S. K., and R. Hajra (2009), Electrojet control of ambient ionization near the crest of the equatorial anomaly in the Indian zone, *Ann. Geophys.*, *27*, 93–105, doi:10.5194/angeo-27-93-2009.

Chakraborty, S. K., R. Hajra, and A. DasGupta (2012), Ionospheric scintillation near the anomaly crest in relation to the variability of ambient ionization, *Radio Sci.*, *47*, RS2006, doi:10.1029/2011RS004942.

Chandra, H., and R. G. Rastogi (1974), Geomagnetic storm effects on ionospheric drifts and the equatorial Es over the magnetic equator, *Indian J. Radio Space Phys.*, *3*, 332–336.

Chandra, H., A. N. Janve, G. Sethia, and R. G. Rastogi (1979), Equatorial *F* region counter electrojet, *Indian J. Radio Space Phys.*, *8*, 1–5.

Chapman, S. (1951), The equatorial electrojet as detected from the abnormal electric current distribution above Huancayo, Peru and elsewhere, *Meteorol. Atmos. Phys.*, *4*, 368–390, doi:10.1007/BF02246814.

Cowling, T. G. (1933), The electrical conductivity of an ionized gas in the presence of a magnetic field, *Mon. Not. R. Astron. Soc.*, *93*, 90–98.

Cowling, T. G., and R. Borger (1948), Electrical conductivity in the ionosphere, *Nature*, *162*, 143, doi:10.1038/162143a0.

Dabas, R. S., L. Singh, D. R. Lakshmi, P. Subramanyam, P. Chopra, and S. C. Garg (2003), Evolution and dynamics of equatorial plasma bubbles: Relationships to $\boldsymbol{E} \times \boldsymbol{B}$ drift, postsunset total electron content enhancements, and equatorial electrojet strength, *Radio Sci.*, *38*(4), 1075, doi:10.1029/2001RS002586.

DasGupta, A., A. Maitra, and S. K. Das (1985), Post-midnight equatorial scintillation activity in relation to geomagnetic disturbances, *J. Atmos. Terr. Phys.*, *47*, 911–916, doi:10.1016/0021-9169(85)90067-4.

Deshpande, M. R., et al. (1977), Effect of electrojet on total electron content of the ionosphere over the Indian sub-continent, *Nature*, *267*, 599–600, doi:10.1038/267599a0.

Duncan, R. A. (1960), The equatorial *F* region of the ionosphere, *J. Atmos. Terr. Phys.*, *18*, 89–100, doi:10.1016/0021-9169(60)90081-7.

Farley, D. T., E. Bonelli, B. G. Fejer, and M. F. Larsen (1986), The prereversal enhancement of the zonal electric field in the equatorial ionosphere, *J. Geophys. Res.*, *91*, 13,723–13,728, doi:10.1029/JA091iA12p13723.

Gouin, P. (1962), Reversal of the magnetic daily variations at Addis Ababa, *Nature*, *193*, 1145–1146, doi:10.1038/1931145a0.

Gouin, P., and P. N. Mayaud (1967), The possible existence of a "counter-electrojet" in equatorial magnetic latitudes, *Ann. Geophys.*, *23*, 41–47.

Haerendel, G., and J. V. Eccles (1992), The role of the equatorial electrojet in the evening ionosphere, *J. Geophys. Res.*, *97*, 1181–1192, doi:10.1029/91JA02227.

Hajra, R., and S. K. Chakraborty (2011), Equatorial ionospheric responses in relation to the occurrence of main phase of intense geomagnetic storms in the local dusk sector, *J. Atmos. Sol. Terr. Phys.*, *73*, 760–770, doi:10.1016/j.jastp.2011.02.014.

Hajra, R., S. K. Chakraborty, and A. Paul (2009), Electrodynamical control of the ambient ionization near the equatorial anomaly crest in the Indian zone during counter-electrojet days, *Radio Sci.*, *44*, RS3009, doi:10.1029/2008RS003904.

Hajra, R., S. K. Chakraborty, and A. DasGupta (2010), Ionospheric effects near the magnetic equator and the anomaly crest of the Indian longitude zone during a large number of intense geomagnetic storms, *J. Atmos. Sol. Terr. Phys.*, *72*, 1299–1308, doi:10.1016/j.jastp.2010.09.015.

Hari, S. S., K. S. Viswanathan, K. S. V. Subbarao, and B. V. Krishna Murthy (1996), Equatorial E and F region zonal electric fields in the post-sunset period, *J. Geophys. Res.*, *101*, 7947–7949, doi:10.1029/95JA03855.

Kelley, M. C., R. R. Ilma, and G. Crowley (2009), On the origin of pre-reversal enhancement of the zonal equatorial electric field, *Ann. Geophys.*, *27*, 2053–2056, doi:10.5194/angeo-27-2053-2009.

MacDougall, J. W. (1969), The equatorial ionospheric anomaly and the equatorial electrojet, *Radio Sci.*, *4*, 805–810, doi:10.1029/RS004i009p00805.

Martyn, D. F. (1955), Geomagnetic anomalies of the F_2 region and their interpretation, in *The Physics of the Ionosphere*, pp. 260–264, Phys. Soc., London.

Maruyama, T. (1988), A diagnostic model for equatorial spread F: 1. Model description and application to electric field and neutral wind effects, *J. Geophys. Res.*, *93*, 14,611–14,622, doi:10.1029/JA093iA12p14611.

Maruyama, T., and N. Matuura (1984), Longitudinal variability of annual changes in activity of equatorial spread F and plasma bubbles, *J. Geophys. Res.*, *89*, 10,903–10,912, doi:10.1029/JA089iA12p10903.

Mendillo, M., J. Baumgardner, X. Q. Pi, P. J. Sultan, and R. T. Tsunoda (1992), Onset conditions for equatorial spread F, *J. Geophys. Res.*, *97*, 13,865–13,876, doi:10.1029/92JA00647.

Ossakow, S. L. (1981), Spread-F theories–A review, *J. Atmos. Terr. Phys.*, *43*, 437–452, doi:10.1016/0021-9169(81)90107-0.

Prakash, S., D. Pallamraju, and H. S. S. Sinha (2009), Role of the equatorial ionization anomaly in the development of the evening prereversal enhancement of the equatorial zonal electric field, *J. Geophys. Res.*, *114*, A02301, doi:10.1029/2007JA012808.

Raghavarao, R., P. Sharma, and M. R. Sivaraman (1978), Correlation of the ionization anomaly with the intensity of the electrojet, *Space Res.*, *XVIII*, 277–289.

Raghavarao, R., M. Nageswararao, J. H. Sastri, G. D. Vyas, and M. Sriramarao (1988), Role of equatorial ionization anomaly in the initiation of equatorial spread F, *J. Geophys. Res.*, *93*, 5959–5964, doi:10.1029/JA093iA06p05959.

Rajaram, G., and R. G. Rastogi (1974), Low latitude *F* region anomalies & the equatorial electric field, *Indian J. Radio Space Phys.*, *3*, 323–331.

Rama Rao, P. V. S., S. Gopi Krishna, K. Niranjan, and D. S. V. V. D. Prasad (2006), Temporal and spatial variations in TEC using simultaneous measurements from the Indian GPS network of receivers during the solar activity period of 2004–2005, *Ann. Geophys.*, *24*, 3279–3292, doi:10.5194/angeo-24-3279-2006.

Rastogi, R. G. (1974), Westward equatorial electrojet during daytime hours, *J. Geophys. Res.*, *79*, 1503–1512, doi:10.1029/JA079i010p01503.

Saito, S., and T. Maruyama (2006), Ionospheric height variations observed by ionosondes along magnetic meridian and plasma bubble onsets, *Ann. Geophys.*, *24*, 2991–2996, doi:10.5194/angeo-24-2991-2006.

Sastri, J. H. (1998), On the development of abnormally large postsunset upward drift of equatorial F region under quiet geomagnetic conditions, *J. Geophys. Res.*, *103*, 3983–3991, doi:10.1029/97JA02649.

Sethia, G., R. G. Rastogi, M. R. Deshpande, and H. Chandra (1980), Equatorial electrojet control of the low latitude ionosphere, *J. Geomagn. Geoelectr.*, *32*, 207–216, doi:10.5636/jgg.32.207.

Sreeja, V., C. V. Devasia, S. Ravindran, and T. K. Pant (2009), Observational evidence for the plausible linkage of equatorial electrojet (EEJ) electric field variations with the post sunset *F* region electrodynamics, *Ann. Geophys.*, *27*, 4229–4238, doi:10.5194/angeo-27-4229-2009.

Sridharan, R., D. Pallam Raju, R. Raghavarao, and P. V. S. Ramarao (1994), Precursor to equatorial spread-F in OI 630.0 nm dayglow, *Geophys. Res. Lett.*, *21*, 2797–2800, doi:10.1029/94GL02732.

Su, S.-Y., C. K. Chao, and C. H. Liu (2008), On monthly/seasonal/longitudinal variations of equatorial irregularity occurrences and their relationship with the postsunset vertical drift velocities, *J. Geophys. Res.*, *113*, A05307, doi:10.1029/2007JA012809.

Su, S.-Y., C. K. Chao, and C. H. Liu (2009), Cause of different local time distribution in the postsunset equatorial ionospheric irregularity occurrences between June and December solstices, *J. Geophys. Res.*, *114*, A04321, doi:10.1029/2008JA013858.

Sultan, P. J. (1996), Linear theory and modeling of the Rayleigh-Taylor instability leading to the occurrence of equatorial spread F, *J. Geophys. Res.*, *101*, 26,875–26,891, doi:10.1029/96JA00682.

Thampi, S. V., S. Ravindran, T. K. Pant, C. V. Devasia, P. Sreelatha, and R. Sridharan (2006), Deterministic prediction of post-sunset ESF based on the strength and asymmetry of EIA from ground based TEC measurements: Preliminary results, *Geophys. Res. Lett.*, *33*, L13103, doi:10.1029/2006GL026376.

Uemoto, J., T. Maruyama, S. Saito, M. Ishii, and R. Yoshimura (2010), Relationships between PRE-sunset electrojet strength, pre-reversal enhancement and equatorial spread-F onset, *Ann. Geophys.*, *28*, 449–454, doi:10.5194/angeo-28-449-2010.

Valladares, C. E., S. Basu, K. Groves, M. P. Hagan, D. Hysell, A. J. Mazzella Jr., and R. E. Sheehan (2001), Measurement of the latitudinal distribution of TEC during ESF events, *J. Geophys. Res.*, *106*, 29,133–29,152, doi:10.1029/2000JA000426.

Woodman, R. F., and C. LaHoz (1976), Radar observations of F region equatorial irregularities, *J. Geophys. Res.*, *81*, 5447–5466, doi:10.1029/JA081i031p05447.